

Committee 1  
Symmetry in Its Various Aspects:  
Search for Order in the Universe

Draft – February 1, 2000  
For Conference Distribution Only



Symmetry and Sidedness in Human Anatomy

Michael K. Atalay  
Instructor in Radiology  
Johns Hopkins Hospital  
Baltimore, Maryland

The Twenty-second International Conference on the Unity of the Sciences  
Seoul, Korea February 9-13, 2000

## Introduction

On the surface, humans, like most vertebrates, demonstrate mirror image symmetry about their midlines. But probe more deeply and symmetry is lost: what holds for the musculoskeletal system is essentially lost in the viscera. Any elementary school child has a rudimentary knowledge of this asymmetry, and—when prompted to Pledge Allegiance—will show you that her heart lies on the left. Yet for a few of us, our heart is not on the left, but rather on the right ... or even midline! Moreover, complete reversal of all torso contents, including abdominal viscera, is occasionally seen. In some individuals, there may be no laterality at all, but virtual mirror image symmetry from top to bottom. While these various permutations represent a small fraction of living humans, they have drawn a vast amount of attention to the etiology of laterality. How and why does visceral left-right (L-R) laterality develop? What gives rise to L-R reversal? Is it genetic or acquired and what are the clinical implications?

Visceral sidedness is determined during the first ~16 days of human embryogenesis, yet the earliest morphologic evidence of asymmetry is not perceivable until several days later. Although the mystery of laterality in vertebrates continues to unfold, much is currently known about the etiology and genetics of normal L-R asymmetry. Many of the genes and events involved in the breaking of embryonic symmetry have been characterized. This paper discusses internal asymmetries of human anatomy, including why they develop and some of the abnormalities that can occur. Human lateralization defects come in a variety of flavors and range in clinical significance from essentially benign to life threatening. These conditions and their associated radiographic findings are presented.

## Normal Anatomy

It is instructive at the outset to review normal human anatomy and relevant terminology.

### **Anatomic axes:**

The three primary axes that are used for anatomical localization are anterior-posterior, dorsal-ventral, and left-right. Anterior refers to the direction an organism is facing when it is in its so-called 'anatomic' position which for a human is standing upright, facing straight ahead. Dorsal is the backside of the body or the side on which the spine is found. Posterior and ventral are the respective opposite directions. Left and right are defined in a natural way by the other two axes, based on the perspective of the organism. For humans, it is easy to see that anterior and ventral are the same, as are posterior and dorsal. For a quadruped, such as a horse, anterior-posterior and ventral-dorsal axes are orthogonal.

### **Normal Human Anatomy:**

The heart is an appropriate beginning for a report on human laterality because in all vertebrates cardiac looping during early embryological development offers the first morphologic glimpse of left-right asymmetry. It is also an organ of primary focus in lateralization disorders because the heart is quite sensitive to L-R axis perturbations and may exhibit a wide variety of congenital defects.

The normal heart is obliquely situated in the anterior portion of the lower thorax with its center of mass and apex lying to the left of the mid-sagittal plane (**Figure 1**). This configuration is referred to as levocardia, literally 'leftward heart.' There are four cardiac chambers: left and right atria (LA & RA) and ventricles (LV & RV). The left and right hearts pump in series with

one another. In normal individuals, venous blood enters the right atrium from superior and inferior vena cavae (SVC & IVC) which are large veins situated just to the right of midline. (Interestingly, during early embryogenesis, the vena cavae are bilaterally symmetric. Asymmetry develops when the left sided vessels regress.) Blood then passes into the right ventricle and is pumped to lungs through the pulmonary arterial system. Pulmonary veins drain oxygenated blood into the left atrium which passes it to the left ventricle. From there it is pumped into the aorta. The aorta promptly arches to the left and gives rise to the great vessels of the head and upper extremities, namely the innominate, left carotid and subclavian arteries. The aorta then descends along the left anterior portion of the spine down through the thorax and into the abdomen. In this manner oxygenated blood is distributed systemically to the various organs of the body. Incidentally, the heart itself is perfused by the coronary arteries which branch immediately off the aorta as it forms above the heart.

In fetal life, gas exchange is achieved by diffusion across the placenta between fetal and maternal blood and not by pulmonary ventilation as of course it is in postnatal life. Fetal lungs are in fact collapsed in the thorax. Fetal pulmonary vascular resistance as a consequence is much higher than in postnatal life, when the lungs are expanded, and is comparable to the higher resistance of the systemic circulation. A result of this is that left and right ventricles see similar afterloads and develop in the fetus in a physiologically comparable manner. Postpartum, however, the work of the left ventricle becomes greater than that of the right and hence morphological differences in ventricular architecture become more pronounced, e.g., asymmetrical hypertrophy of LV versus RV. This augments the 'built-in' asymmetry of embryogenesis.

In addition to the early asymmetry of cardiac development—manifest initially by dextral looping—left and right lungs and airways also develop differently. In contrast to heart asymmetry which evolves from an initially symmetric midline tube, the lungs are never symmetric structures; they originate from asymmetric progenitor cells.<sup>1</sup> Anatomically, the right lung has 3 lobes and 10 segments, the left, 2 lobes and 9 segments (**Figure 1**). The right mainstem bronchus branches proximally to give off the bronchus to the right upper lobe (eparterial bronchus) and the bronchus intermedius which subsequently bifurcates into the bronchi to middle and lower lobes. The left mainstem bronchus, on the other hand, divides more distally to form the bronchi to upper and lower lobes.

Within the abdomen there is also significant asymmetry, most notably the presence of the stomach and spleen in the left upper quadrant, the liver in the right upper quadrant, and the well-characterized rotation of bowel with the ascending colon and duodenum on the right and the descending colon on the left (**Figure 2**).

## Anatomical Asymmetries: Which *situs* It On?

The term *situs* is used to describe the pattern of anatomic organization. It turns out that the left or right atria and respective left or right viscera are almost always on the same side of the body, so *situs* has come to mean *visceroatrial situs*. This is the cornerstone of ‘sidedness’ by which all other structures are judged. So, if the anatomic left atrium is on the right, all other normally left sided structures should also be on the right. This is referred to as concordance. If

---

<sup>1</sup> There are three mechanisms for the development of morphologic asymmetry: (1) initial bilateral symmetry with regression on one side, e.g. vena cavae, (2) initial symmetry with asymmetrical growth, e.g. heart, and (3) asymmetric *de novo* development, e.g. lungs.

this condition is not maintained than discordance exists along with an associated high risk of congenital heart disease and other anomalies.

Because of the high degree of viscerotrial concordance, radiographic evaluation of the abdominal is useful to predict body *situs*. Since the gastric air bubble and the liver are usually readily recognizable structures on an abdominal radiograph, a simple x-ray may provide conclusive information. Tomographic imaging modalities such as MRI and CT offer much greater detail than plain film radiography, but they are much less commonly used in the neonatal population where *situs* abnormalities are often identified. Chest x-ray (CXR) may offer clues, including the presence and location of the minor fissure, which is a right lung structure, as well as the bronchial branching pattern. A normal CXR is shown in **Figure 3**.

There are three *situs* designations. *Situs solitus* refers to the normal condition where the LA, stomach, spleen and aorta are all on the left side of the body and the RA, liver, and IVC are on the right. *Situs inversus* is the mirror image of *situs solitus*. The morphological left structures are on the right and the visa versa. Finally, there is *situs ambiguus* in which the sidedness is not determinable (**Figure 4**). Subsets include left and right isomerism which are discussed below. Usually in this condition the liver and stomach are midline structures. The heart may be in levo-, dextro- (rightward) or meso- (midline) position. Bowel malrotation is typical. This may be diagnosed radiographically by fluoroscopic gastrointestinal evaluation.

### **Situs Inversus Totalis**

*Situs inversus (SI)*, also called *situs inversus totalis*, is by far the most common of the so-called syndromic left-right axis abnormalities. As mentioned above, *SI* is the mirror image of

*situs solitus*, the normal configuration of heart and viscera . Three images of a CT scan from a patient with *SI* are shown in **Figure 5**. It is seen approximately 50% of the time in a condition known as Primary Ciliary Dyskinesia (PCD), also called Immotile Cilia Syndrome (ICS), which is described in greater detail in a subsequent section. The incidence of *SI* ranges from 1/8000 to 1/25000 living persons (1-3) with roughly 1/5-1/4 of cases associated with PCD (3). Radiographic survey suggests that 1/7000 to 1/8000 is an accurate general estimate. In Scandinavia the prevalence is 1/8000 and in the USA approximately 1/11000 (4). These may be underestimates since *SI* by itself may be completely asymptomatic. Of people with *SI*, the exact incidence of cardiac abnormalities is not known, but it appears to be approximately 0.8-5% (5), which may be slightly higher than the general population. The cardiac defects characteristically seen in *SI* are atrioventricular discordance (25%), double-outlet RV (30%), pulmonary stenosis/atresia (50%), ventricular-septal defect (60%), and right sided aortic arch (80%) (1). The inheritance pattern of *SI* appears to be autosomal recessive (3).

### **Kartagener's Syndrome**

Kartagener's syndrome is characterized by the triad of (i) *situs inversus totalis* (including dextrocardia), (ii) paranasal sinusitis/polyposis, and (iii) bronchiectasis in a pattern that often resembles mild cystic fibrosis. Otitis infections are common in younger patients and males may be infertile. As well, anosmia—complete lack of the sense of smell, nasal polyposis, and agenesis of the frontal sinuses occasionally occur. Kartagener's is a subset of PCD. Since *SI* is a criterion, and since 50% of PCD demonstrates *SI*, Kartagener's is approximately half as common as PCD. In fact, the prevalence is estimated to be 1/50000. As with *SI*, very few patients with this disease have significant CHD (1), and there may be only a mild increased risk of other anomalies. Life

expectancy is usually normal. While the syndrome is typically inherited in a recessive manner, autosomal dominant and X-linked inheritance patterns have been observed.

Chronic sinusitis and bronchiectasis are due to a common underlying problem, and in fact the defining characteristic of this syndrome, namely dysmotile cilia. Cilia are described in greater detail below. In brief, they are tiny whiplike cellular appendages that act in synchrony on the surface of epithelial cells to move surrounding fluid. In the airways and sinuses, they serve as a critical first line of defense against microscopic debris, dust and microorganism by aiding in their removal. Impaired ciliary function at this level results in the clinical symptoms of Kartagener's syndrome. As discussed below, there appears to be a remarkable connection between cilia and the determination of laterality.

### Heterotaxia Syndromes

Failure to establish concordant asymmetry of organs along the L-R axis results in heterotaxy, from the Greek for 'other arrangement.' This is any configuration of organs that is not *situs solitus* or *situs inversus*, i.e., *situs ambiguus*. The most extreme form of heterotaxy is isomerism which represents the complete failure to break bilateral symmetry in the developing embryo. The two possible results are bilateral left-sidedness or left isomerism (Ivemark Syndrome) and bilateral right-sidedness or right isomerism. The former condition is also known as polysplenia, deriving from the fact that the spleen is normally on the left. Findings in addition to multiple spleens include bilateral bilobed (left) lungs, biliary atresia, interruption of the IVC with azygos continuation, and intestinal malrotation. Four CT images of a patient with polysplenia are shown in **Figure 6**. Note (a) the presence of multiple small splenules in the right



upper quadrant and (b) the dilated azygos vein with no evidence of an IVC. Polysplenia has a marked female predominance. CHD is present in 90% of cases and demonstrates marked heterogeneity with a variety of clinical implications. Cardiac defects include pulmonary stenosis/atresia (30%), transposition of the great vessels (30%), atrioventricular septal defects (40%), dextrocardia (40%), common atrium (80%), interruption of the IVC with azygos continuation (65-70%), LV outflow tract obstruction (40%), persistent left SVC (40%) and partial anomalous pulmonary venous return (40%) (1).

Bilateral right-sidedness or asplenia is, as expected, associated with the absence of a spleen. As well, there are often bilateral trilobed lungs, bowel malrotation, microgastria, tracheoesophageal fistula, and imperforate anus. The IVC and abdominal aorta are often on the same side of the spine. **Figure 7** is a CXR of a patient with asplenia syndrome. Note the large, mostly symmetric liver shadow. A slight male predominance is seen with this condition, and CHD is almost a certainty (~99-100%) (5). Cardiac lesions can include atrioventricular septal defects (85%), total anomalous pulmonary venous return (70%), transposition of the great vessels (80%), pulmonary stenosis/atresia (80%), dextrocardia (40%), common atrium (90%), persistent left SVC (50%), and monoventricle (50%) (1). Patients frequently present with cyanosis and respiratory distress.

### *Cardiac Malposition*

Cardiac apex position may be on the left (levocardia), the right (dextrocardia), or midline (mesocardia—usually seen with *situs solitus*). Importantly, apical position may be concordant or discordant with the visceratrial *situs*, with the important caveat that discordance is associated with a very high incidence of anomalies. For example isolated dextrocardia with *situs solitus* comes with a 90-95% risk of a congenital heart disease which include atrioventricular

discordance (50%), monoventricle (25%), pulmonary stenosis/atresia (60%), right sided aortic arch (8%) and ventricular septal defect (60%) (1). Its incidence reportedly ranges from 1/7500 to 1/29000 (1). Isolated levocardia with *situs inversus* is very rare and the incidence of intracardiac abnormalities is virtually 100% (1, 5). A CXR of a patient with *situs inversus* and levocardia is shown in **Figure 8**. The presence of levocardia and a right sided gastric bubble are suggestive of this condition. Congenital abnormalities include pulmonary stenosis/atresia (89%), atrioventricular canal (67%), and total anomalous pulmonary venous return (44%) (1).

### *Prognosis*

In general, heterotaxia represents approximately 3% of neonatal cardiovascular malformations and has a 30% mortality rate. It may be, however, that some cardiac perturbations occur in cases of subtle, nondetected L-R axis abnormalities, making 3% a conservative estimate. Right isomerism carries a worse prognosis than left isomerism due mostly to the more severe heart disease and probable immunodeficiency. The mortality rate in the first year of life is 80% and 60%, respectively, for right and left isomerism. Rarely, normal life expectancy may accompany left isomerism.

### *Genetics*

Data indicate that heterotaxy has a strong genetic component and the familial recurrence risk of isomerism is approximately 10%. Autosomal recessive, autosomal dominant and X-linked modes of inheritance have all been implicated. Evidence suggests that a single gene mutation may result in a variety of phenotypes and, conversely, a single phenotype can arise as from different gene abnormalities.

## Primary Ciliary Dyskinesia

Approximately 1 in 25000 people have a condition known as Primary Ciliary Dyskinesia (PCD), also referred to as Immotile Cilia Syndrome (ICS) (4). Kartagener's Syndrome represents a special subset of patients in which the triad of *SI*, bronchiectasis, and chronic sinusitis is present. In fact, the syndrome of PCD grew out of the initial observations regarding Kartagener's syndrome. Radiographically and symptomatically the condition of PCD is similar to a mild form of cystic fibrosis (6).

In 1904 Siewart published a case report of a 21 year old man in whom the 3 elements of the classic triad were present. However, it wasn't until 1933 that M. Kartagener first recognized that these findings represented components of a syndrome (7). Little was offered by way of understanding the condition until 1976, when Bjorn Afzelius reviewed the electron micrographic data of the sperm tails of 3 infertile men having immotile but otherwise normal spermatozoa (8). In addition, all three men had chronic sinusitis and bronchiectasis, and two had *situs inversus*, completing the Kartagener triad. The startling discovery was that a key molecular component of the motor apparatus responsible for sperm motility was missing! Afzelius believed that the pathology was due to a gene with incomplete penetrance and possibly coding for the missing molecular component called dynein or a protein that binds dynein to the ciliary microtubules. He concluded that immotility of cilia (and flagella) played an important role in the clinical presentations. Furthermore, he assumed that "chance alone will determine whether the viscera will take up the normal or the reversed position during embryogenesis when the dynein arms are missing."

Since Afzelius' original publication, much has been learned about Kartagener's syndrome and in turn PCD, most notably that there is vast heterogeneity in the presentation and the underlying genetics characterizing these conditions (4). While the absence of dynein arms is the most common micropathology associated with PCD, there are many different gene mutations that may give rise to dysmotile or immotile cilia, and dynein is not always involved. Other ciliary molecules such as those involving the radial spokes or microtubules may be impaired or missing. Moreover, there appears to be sufficient difference between cilia and flagella that in some instances sperm may be normally motile while cilia of the same man may be dysmotile and visa versa. Of note, however, is that virtually all of the subsets of PCD are characterized by a 50% prevalence of *situs inversus* (4, 6).<sup>2</sup> Hence, essentially 50% of PCD patients have Kartagener's syndrome. As mentioned earlier, *situs inversus* associated with PCD represents ~1/5-1/4 of all cases of *SI*. *Situs ambiguus* is thought to be extremely rare in PCD. However, the incidence of serious abnormalities may be significant; in one study 12% (4/32) of patients with PCD had congenital heart disease and 16% (5/32) had esophageal problems (9). **Figure 13** displays three different forms of abnormal cilia obtained from patients with PCD. In (a) the dynein arms are missing; in (b) the radial spokes are disrupted; and finally, in (c) the central microtubule pair is aberrantly fused.

Until recently the diagnosis of PCD rested on the detection of specific aberrations of nasal and bronchial cilia during electron microscopic evaluation. Now, however, functional methods are available that permit direct assessment of the ciliary transport mechanism (4). In the saccharin test for example, the time for transport of small grains of saccharin from the nasal mucosa to the pharynx is measured. The most reliable test is one in which cells from a nasal

---

<sup>2</sup> At least 2 subgroups of PCD are not characterized by equal proportions of *SI* and *SS*. These include the

epithelium biopsy specimen are separated out and cultivated in a culture solution. After a few days, native cilia are shed and a new population emerges. Normal rotation of isolated cells or cell aggregates in the surrounding fluid bath suggests normal coordinated beating of cilia. Non-rotation corresponds to the presence of immotile cilia.

## Microbiology of Cilia (10)

Cilia are tiny hair-like cellular appendages ( $\sim 0.25 \mu$  diameter x  $6 \mu$  length) constructed from cytoskeletal filaments called microtubules (**Figure 9**). The primary function of cilia is to move fluid across a cell's surface or, in the case of a flagellum, to propel single cells through fluid. Cilia are found abundantly throughout human epithelium. In particular, the human respiratory mucosa consists of a very high density of cilia ( $\sim 10^9/\text{cm}^2$ ) which in a coordinated manner act to sweep layers of secreted mucus along with trapped dust particles, microbes, and sloughed cells from the airway to the oropharynx where they can be expectorated or swallowed. Cilia located in the paranasal sinuses serve a similar purpose. Ciliated epithelia are also present in the Eustachian tubes where they help to propel middle ear fluid, again into the oropharynx. As well, cilia lining the fallopian tubes aid in the passage of ova, and flagella, which are closely related to cilia but much longer ( $\sim 50 \mu$ ), provide a rhythmic force necessary for the propulsion of sperm. The ventricular ependymal cells of the brain are also ciliated; however, their presence may be vestigial since they are not required for normal cerebrospinal fluid production or flow.

---

group who lack cilia and the group whose cilia are missing the central microtubule pair (4).

## Ciliary Movement

The movement of a cilium is similar to that of a whip and is depicted in **Figure 10**. A power stroke is performed as the fully extended cilium moves against the surrounding fluid; this is followed by a recovery phase in which the cilium—folded on itself to reduce its viscous drag—unrolls into its initial position. Fields of cilia demonstrate synchronized movement that results in coordinated wave patterns that can be visualized microscopically. A flagellum on the other hand, while structurally similar to a cilium but much longer, oscillates in a quasi-sinusoidal manner to achieve cell propulsion.

The movement of a cilium or flagellum is achieved by the bending of a continuous core structure of microtubules known as the axoneme whose length may extend from 10  $\mu$  up to 200  $\mu$ . A microtubule is a long hollow tube of protein with an outer diameter of ~25 nm and an inner diameter of ~14 nm. The appearance is slightly modified in an axoneme where nine special doublet microtubules spiral in a ring around a central pair of single complete microtubules in a so-called '9+2' array (**Figure 11**). The doublets consist of one complete (A) and one partial (B) microtubule fused along a common wall. On cross-section the complete microtubule has 13 distinct subunits called tubulin. The partial microtubule has 11 subunits. The tubulin subunits coalesce in the axial direction to form linear strands called protofilaments (**Figure 12**). Each tubulin molecule (~8 nm) is itself a heterodimer comprising two related globular protein subunits labeled  $\alpha$ - and  $\beta$ -tubulin, each consisting of approximately 450 amino acids. These subunits are highly conserved in evolution, possibly reflecting the architectural constraints brought about by the large number of different proteins to which they bind. As a microtubule forms, the  $\beta$  ends of one row attach to the  $\alpha$  end of the next row, conferring polarity to the growing structure.

In order for the axoneme to bend, linking molecules are present between successive microtubules doublets. Dynein, a large protein complex containing 2 or 3 globular heads with thin stalks, forms outer and inner arms connecting one A tubule to the adjacent B tubule. The separation between dynein arms from one level to the next is fixed at 24 nm. As seen from the base of the axoneme, the dynein arms extend from Tubule A in a clockwise direction. This confers chirality to the cilium which in turn determines the manner in which it moves. The dynein molecules are essential for the proper functioning of the cilium. In the presence of ATP, the primary cellular energy substrate, the dynein arms attached to one A tubule 'walk' along the neighboring B tubule towards the base or 'minus' end. The mechanism is similar to that seen between myosin and actin filaments in skeletal muscle. Without cross-links to hold the doublets in place relative to one another, the action of the dynein molecules would result in the sliding of one doublet past the other. Consequently, thin links called nexin tether the doublets, offering a restoring force and resisting sliding between adjacent doublets. The result is that the axoneme bends. Nexin links occur at more widely spaced intervals (~86 nm).

Importantly, poorly understood protein-protein interactions transmitted along the axoneme are necessary for the production of a bend instead of a simple twist which would result if all axonemal dynein became active at the same time. In addition to dynein and nexin, spoke molecules spaced at intervals of 29 nm extend radially from a sheath surrounding the two central microtubules to the outer doublets. These molecules are involved in the regulation of the ciliary beat. In total, there are at least 130 different polypeptide species used in the construction of a ciliary axoneme.

### **Ciliary Formation**

Centrioles are small cylindrical organelles (0.2 x 0.4 microns) within cells that serve as templates for the formation of cilia and flagella. The walls of centrioles are formed by 9 microtubule fused triplets. As with the axoneme, only one constituent microtubules in each set is complete; the other two are partial and provide a 'piggyback' appearance on micrograph (**Figure 12**). The triplets confer a 40° rotational symmetry. Axonemal doublets grow from two of the three microtubules in each triplet. Tubulin dimers and other proteins add to the growing or 'plus' end of the axoneme. The origin of the central pair of complete microtubules in the cilium is unclear, as there is no central pair in centrioles.

Although under special circumstances centrioles can develop *de novo*, the vast majority arise from pre-existing centrioles.

## Embryological development of laterality

Early in embryogenesis the primary axes of orientation are developed. Initially, anterior-posterior (A-P) and dorsal-ventral (D-V) axes form, followed by the L-R axis. All of these are linked to multiple genetic steps. Important information regarding the orientation of A-P and D-V axes comes from the egg and the event of fertilization. The egg possesses inherent asymmetry: one half—the vegetal pole—contains mostly nutrient material, and the other half—the animal pole—contains the genetic material. This asymmetry generates one axis. Fertilization of the egg by a sperm occurs at some site on the egg surface. This action generates hemispheric polarity, yielding a second orthogonal axis. Roughly speaking, these orientations correlate to A-P and D-V axes. L-R axis orientation is in part dependent on proper formation of the other axes (1).



Although events within the first 16 days post fertilization set the stage for laterality in human embryology, cardiac looping, which occurs at day 23, is the earliest morphologic event to display L-R asymmetry (1). Before this the ventral midline cardiac tube, which appears at day 20 and which is composed of cells migrating from the cardiac primordia located in both halves of the embryo, is essentially morphologically symmetric. (Evidence suggests, however, that the migrating primordial cardiac cells acquire different information on left and right sides (11).) Cardiac looping provides a spatial context for normal cardiac development and loop defects can result in complex structural heart abnormalities. Presently, the morphogenetic mechanisms responsible for initiating cardiac looping are unknown. Cardiovascular lateralization is thought to confer a measure of circulatory efficiency and complexity that provides evolutionary advantage to vertebrates. The same is probably also true for asymmetry in the gastrointestinal system which occurs later in embryological development.

The question arises as to how in the first few days of embryogenesis symmetry at the cellular level is broken. It appears that cell-cell and cell-extracellular matrix interactions are crucial for establishing sidedness (1). A number of genes and molecular markers have been described in association with very early embryological asymmetry in various animal models such as chicks, mice, and *xenopus* (frog) (2, 3, 12-15). In most cases, these markers are expressed asymmetrically over some period of embryonic development. Detailed discussion of these genetic factors is outside the scope of this paper. However, it is noted that there appear to be at least a few asymmetrically expressed markers that are conserved across species. RNA's encoding proteins such as *lefty* and *nodal* from the superfamily known as transformation growth factor  $\beta$  (TGF- $\beta$ ) have been detected in mouse, chick, and frog embryos. Importantly, the earliest differential marker expression occurs in a small ciliated region of the developing embryo referred

to as the embryonic node.<sup>3</sup> Manipulation of the expression or distribution of several of these genes and markers results in curious aberrations of laterality. Some manipulations, particularly those involving the embryonic node, result in randomization of the direction of cardiac looping or of body *situs* in general (1).

Mouse models of lateralization abnormalities have been developed. The most extensively studied mutant model is the *iv* or *inversus viscerum* mouse which has features that are very similar to the condition of Primary Ciliary Dyskinesia in humans. The genetic defect is located on mouse chromosome 12, corresponding to a human locus on chromosome 14, and behaves as a recessive trait. The gene product is ‘left-right dynein,’ or LRD, which is an axonemal dynein (2). Heart looping abnormalities and congenital heart disease have a relatively high incidence in this model. Remarkably, homozygous animals have an equal chance of *situs inversus* and of *situs solitus*. (The fraction of the total that are *situs ambiguus* depends on the strain and ranges from 3-40% (2).) This suggests that the absence of a functional gene in the *iv* locus results in randomization of laterality—just as with the human condition. In other words, rather than a gene for *situs solitus* and a gene for *situs inversus*, there appears to be a gene for which one allele in both single or double copy (hetero- or homozygous) will result in *situs solitus*. This is the ‘functional’ allele. The other allele for this gene, i.e., the one in the *iv* mouse, cannot control laterality and hence results in random L-R asymmetry (16). In his paper entitled “Inheritance of Randomness” Afzelius (17) explains how such an argument could also be used to explain the prevalence of left-handedness and possibly even homosexuality.<sup>4</sup>

---

<sup>3</sup> The embryonic node is called Spemann’s (or dorsal) organizer in *Xenopus* and Henson’s Node in chicks. Nodal cells ingress during the gastrulation phase of embryogenesis and form the notochord.

<sup>4</sup> Approximately 8% (159/1993) of the population born to 2 right-handed parents are left-handed, approx. 20% (34/174) born to one right- and one left-handed parent are left-handed, and approx. 55% (6/11) born to 2 left-handed parents are left-handed (18). According to this balanced polymorphism model,

Okada *et al* (14), using videomicroscopy, have very recently demonstrated that in normal mice, embryonic nodal cilia act in a coordinated manner to efficiently move overlying fluid in a right to left direction. In contrast, however, the nodal cilia of the mouse *inv* model are immotile and fluid flow over the node is absent. Their rather compelling hypothesis which is supported by their data is that nodal cilia play a key role in the L-R axis determination. Their data “suggest that the normal, rapid leftward nodal flow is essential for the proper L-R body axis determination.” Furthermore, leftward normal nodal flow appears to be the first determinant of L-R body axis. According to their theory, a morphogen, known or unknown, that is secreted into the extraembryonic fluid would be preferentially swept towards the left, thereby creating an L-R chemical gradient that could serve as a precursor to morphologic lateralization.

Interestingly, another mouse model exists in which mutation of the *inv* gene (for inversion of embryonic turning) results in a high percentage of *situs inversus* animals. The gene has yet to be characterized. As with the *iv* gene, this *inv/inv* homozygous mutation changes the behavior of embryonic nodal cilia (14). However, contrary to the expected finding of nodal flow reversal, flow direction is normal, but the magnitude is significantly slower than normal. If the Okada hypothesis is correct then it would seem that the *rate* of nodal flow—and not simply the direction—is a critical factor in L-R determination.

Afzelius (19) has also provided evidence “for the opinion that cilia in the early embryo, by their work, determine the laterality of the body; without cilia body laterality would be

---

there is a functional allele *A* that determines right-handedness and a non-functional allele *a* that exerts no effect on handedness. A right-handed person may have *AA*, *Aa*, *aA*, or *aa* alleles and a left-handed person has *aa*. Hence, if *A* and *a* are found in equal proportions, for 2 right-handed parents the probability of having *aa* is  $3/7 \cdot 3/7$  or  $9/49$ , of which 50% or  $9/98$  (10%) will be left-handed. Similarly, for one right and one left-handed parent the chance for *aa* is  $3/7 \cdot 1/1$ , of which 50% or  $3/14$  (21%) will be left-handed. Finally, for 2 left-handed parents, the chance of a left-handed child is clearly 50%. These values are all in good agreement with the data.

randomized.” In particular, he posits that the monocilia located in the primitive node are directly responsible. These monocilia have a ‘9+0’ arrangement of microtubules; while the outer doublets are all present, the center pair of singlets seen in usual cilia is absent. By virtue of the clockwise attachment of the dynein arms as viewed from the base, these monocilia are endowed with chirality. This in turn determines the direction of rotation of the cilia and subsequently the direction of water flow over the node. Afzelius in essence supports the data and conclusions of Okada *et al.* It should be noted that other authors argue that the embryonic node acts more as a relay of L-R orientation than as a source (2).

## Conclusions

This paper reviews many of the lateralization defects that can occur in humans and other animals and their clinical and radiological manifestations. Specifically, the concepts of *situs inversus* and heterotaxia are presented as potential variations from the normal *situs solitus*. The clinical implications of these various abnormalities range from essentially benign as with *situs inversus* to potentially lethal, e.g., right isomerism. Our current understanding of visceral lateralization comes largely from the study of embryogenesis in other vertebrate species. Frog, mouse, and chick embryos in particular have demonstrated multiple molecular L-R asymmetries early in development. Several RNA's and proteins are found in unequal concentrations in left and right halves at various phases of embryogenesis. Some of these so-called markers appear to be conserved across species.

Although dextral looping of the cardiac tube during the neurulation period offers the first sign of morphologic L-R asymmetry, the earliest evidence of molecular asymmetry occurs around small pocket of ciliated tissue generically referred to as the embryonic node. Compelling data implicate this ciliated apparatus as a major player in the determination of L-R laterality. In normal subjects where the cilia create a general leftward nodal flow, *situs solitus* develops. When the cilia are impaired, however, reversal of body *situs* is observed with the same frequency as normal *situs*. For humans, this condition is referred to as Primary Ciliary Dysmotility (PCD) or Immotile Cilia Syndrome (ICS). Generally speaking, PCD is accompanied by abnormalities in the ciliary function at all stages of life, which in turn result in a variety of clinical manifestations including recurrent sinus and middle ear infections, bronchiectasis, anosmia, and male infertility. Interestingly, PCD is considered to be significantly less common than pure *situs inversus*. There are a few explanations that may account for this. First, the embryonic node may be very sensitivity to ciliary disturbances, thereby setting a lower threshold to laterality disturbances than to pathologic manifestations in other areas of the body. Alternatively, since cilia in the embryonic node are known to be slightly different in ultrastructure than cilia elsewhere in the body, it is possible that functional defects in nodal cilia are more profound or are manifest differently than in '9+2' cilia.

A physiological mechanism for the prominent role of cilia in the establishment of L-R asymmetry is provided by a model in which some probably unknown morphogen that is initially symmetrically distributed in the embryonic milieu is swept by the cilia from right to left. A concentration gradient is thus established from which a host of mechanisms can act to provide positive feedback for asymmetrical development, most notably gene expression. The leftward

nodal flow is itself due to the specific chirality of dynein attachments in ciliary architecture. The factors responsible for this particular ultrastructure are incompletely understood.

Explanations for the development of heterotaxy may also involve embryonic node cilia. Other factors such as the timing of asymmetric gene expression and the coordination of extracellular matrix events with alterations in cell shape are probably also responsible. The generation of proper L-R orientation requires two distinct mechanisms. First, there must be a process which generates L-R asymmetry. Second, a mechanism must be in place for appropriate alignment with the other embryonic axes. These mechanisms, which remain incompletely understood, may be distinct or interdependent, but in principle it is the former that goes awry in heterotaxy abnormalities.

## Figures

**Figure 1.** Painting depicting normal thorax. L/RV: left/right ventricle; RA: right atrium. S/IVC: superior/inferior vena cava; Ao: aorta; PA: pulmonary artery; L/RL: left/right lung.

**Figure 2.** Painting depicting normal upper abdomen.

**Figure 3.** Normal chest x-ray.

**Figure 4.** Schematics of *situs solitus*, *situs inversus* and two forms of *situs ambiguus* (right and left isomerism). eb: eparterial bronchus. SP: spleen. ST: stomach. AZY: azygos vein.

**Figure 5.** Three images from a non-contrast CT scan of a patient with *situs inversus*. MPA: main pulmonary artery.

**Figure 6.** Four images from a contrast CT scan of a patient with left isomerism.

**Figure 7.** CXR of a patient with right isomerism.

**Figure 8.** CXR of a patient with abdominal *situs inversus* and levocardia.

**Figure 9.** Electron micrographs of cilia on cross-section and parallel to the long axis.

**Figure 10.** Depiction of the motion of cilia and flagella.

**Figure 11.** Schematic of the cross-section of a cilium with a similar view of an electron micrograph.

**Figure 12.** Schematic of the architecture of a microtubule, ciliary doublet, and centriole.

**Figure 13.** Electron micrographs demonstrating various ciliary defects seen in PCD. Details are provided in the text.

1. P. Bowers, M. Brueckner, H. Yost, *Semin Perinatol* **20**, 577 (1996).
2. M. Mercola, *Semin Cell Dev Biol* **10**, 109 (1999).
3. B. Casey, *Hum Mol Genet* **7**, 1565 (1998).
4. B. Afzelius, *Thorax* **53**, 894 (1998).
5. W. Dahnert, *Radiology review manual* (Williams & Wilkens, Baltimore, ed. 3rd, 1999).
6. H. Nadel, D. Stringer, H. Levison, J. Turner, J. Sturgess, *Radiology* **154**, 651 (1985).
7. M. Kartagener, *Beitr Lin Tuberk* **83**, 489 (1933).
8. B. Afzelius, *Science* **193**, 317 (1976).
9. V. Engesaeth, J. Warner, A. Bush, *Pediatr Pulmonol* **16**, 9 (1993).
10. B. Alberts *et al.*, in *Ciliary movement* . (Garland Publishing, NY, NY, 1989) pp. 644.
11. C. Hoyle, N. Brown, L. Wolpert, *Development* **115**, 1071 (1992).
12. D. Supp, M. Brueckner, S. Potter, *Semin Cell Dev Biol* **9**, 77 (1998).
13. I. Varlet and E. Robertson, *Curr Opin Genet Dev* **7**, 519 (1997).
14. Y. Okada *et al.*, *Mol Cell* **4**, 459 (1999).
15. E. Robertson, *Science* **275**, 1280 (1997).
16. W. J. Layton, *J Hered* **67**, 336 (1976).
17. B. Afzelius, *Med Hypotheses* **47**, 23 (1996).
18. D. Rife, *Genetics* **25**, 178 (1940).
19. B. Afzelius, *Int J Dev Biol* **43**, 283 (1999).



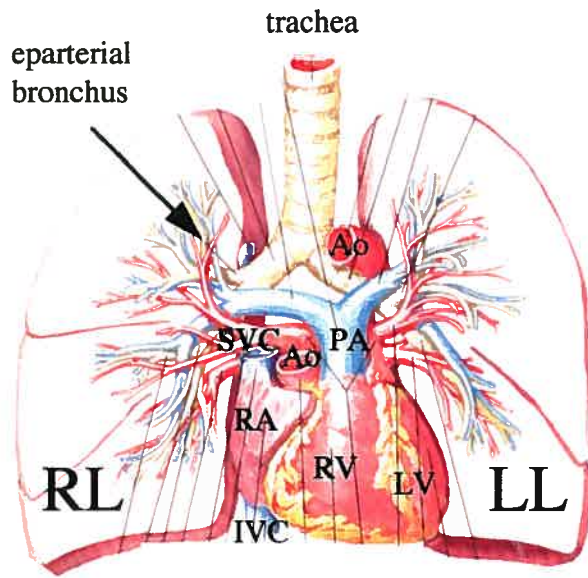


Figure 1

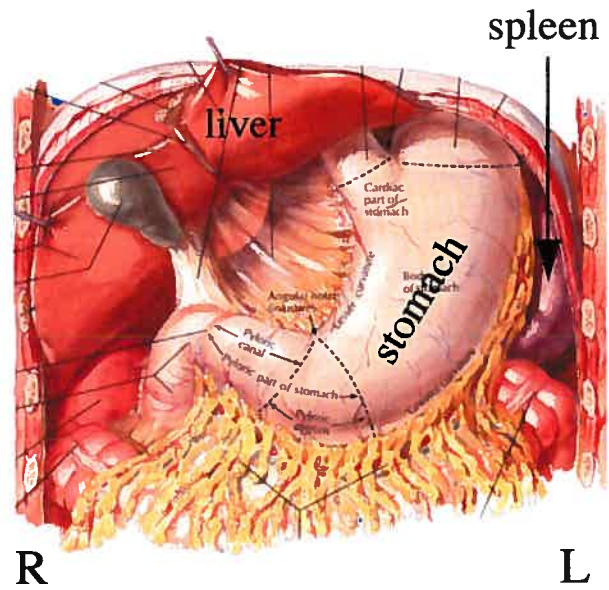


Figure 2

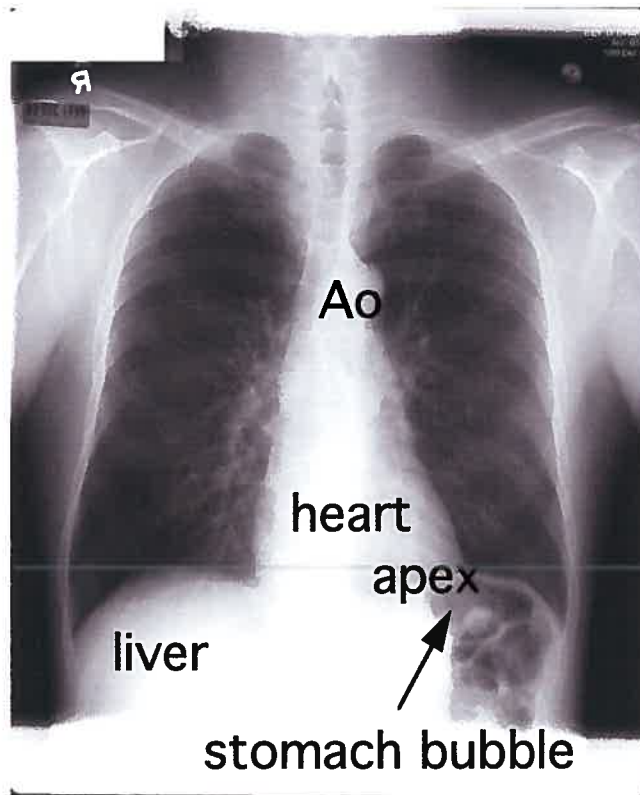
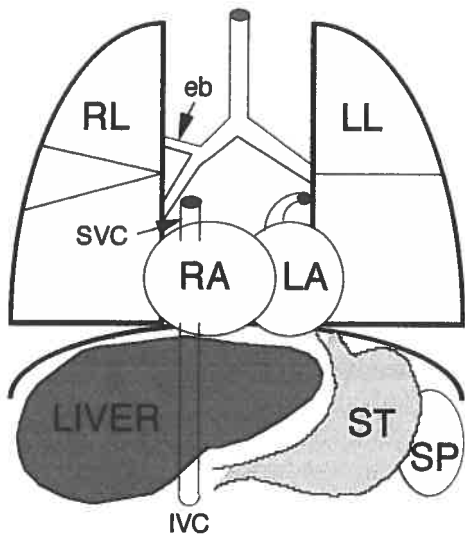
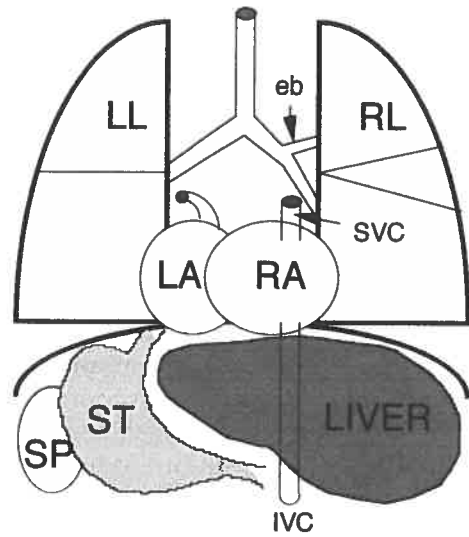


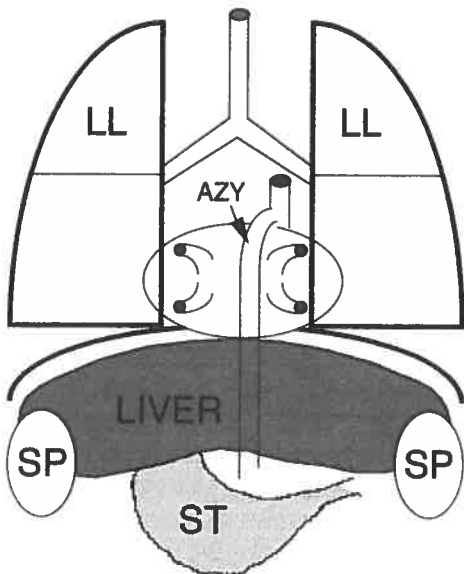
Figure 3



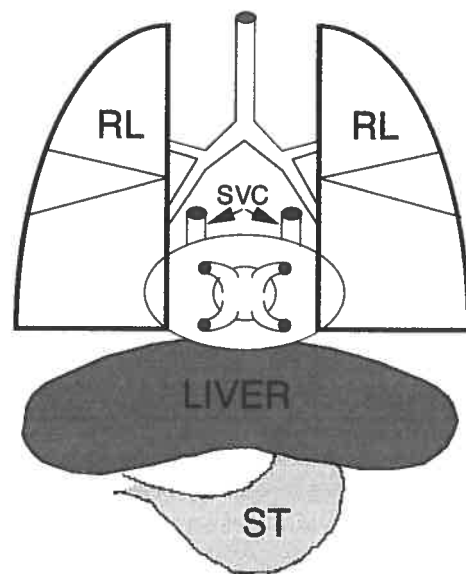
**SITUS SOLITUS**  
ANTERIOR VIEW



**SITUS INVERSUS**  
ANTERIOR VIEW



**LEFT ISOMERISM**  
POSTERIOR VIEW



**RIGHT ISOMERISM**  
POSTERIOR VIEW

Figure 4

Figure 5

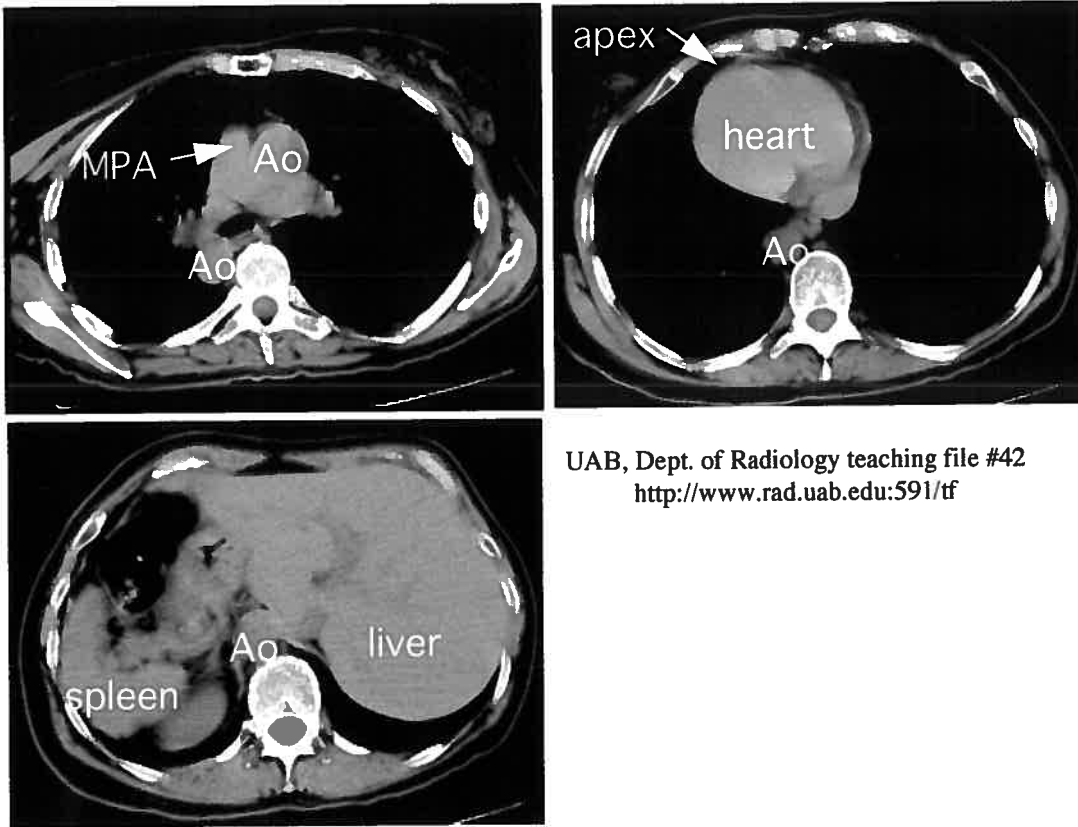
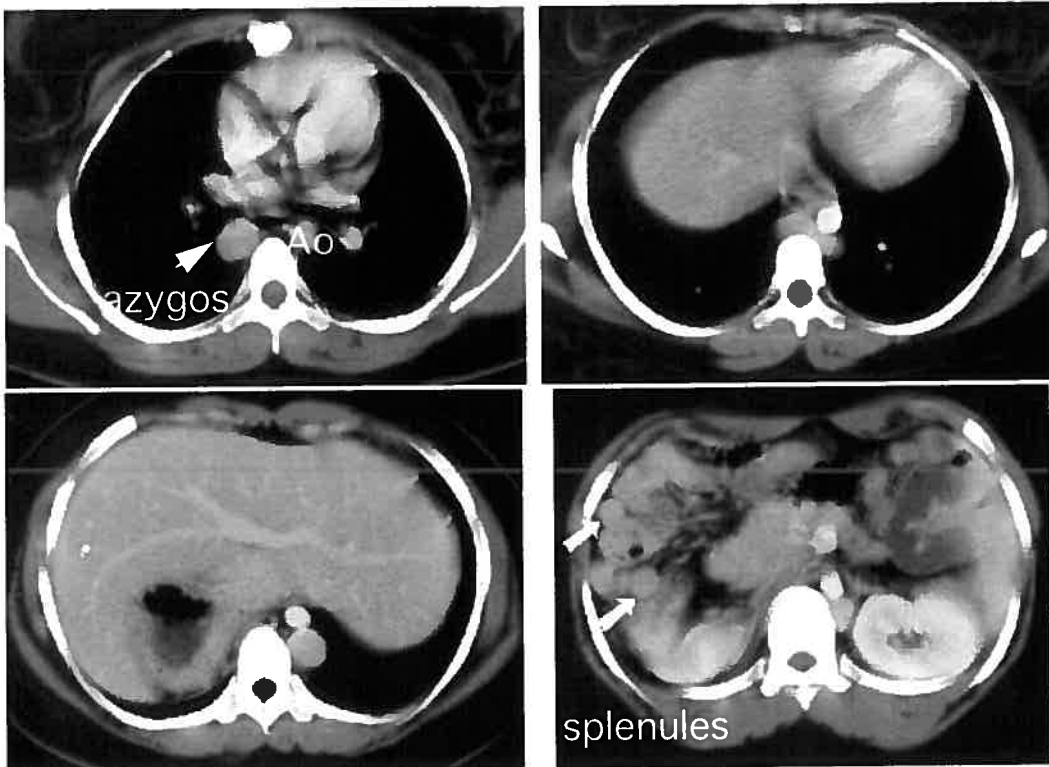


Figure 6



Univ. Hospitals of Cleveland, Dept. of Radiology teaching file #173  
<http://www.uhrad.com/ctarc>

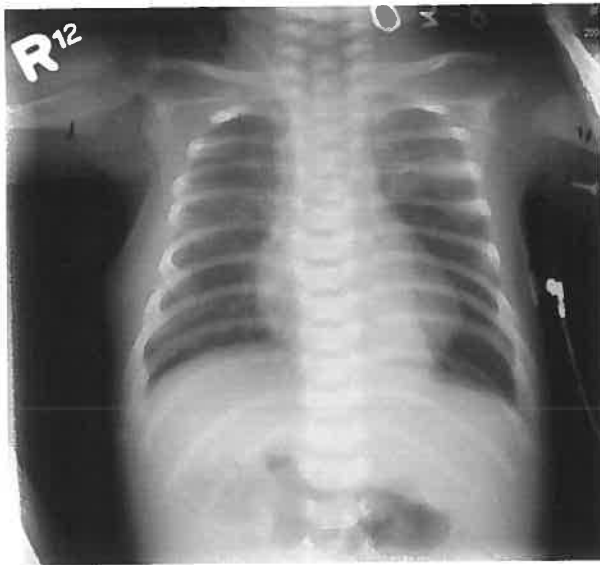


Figure 7



Figure 8

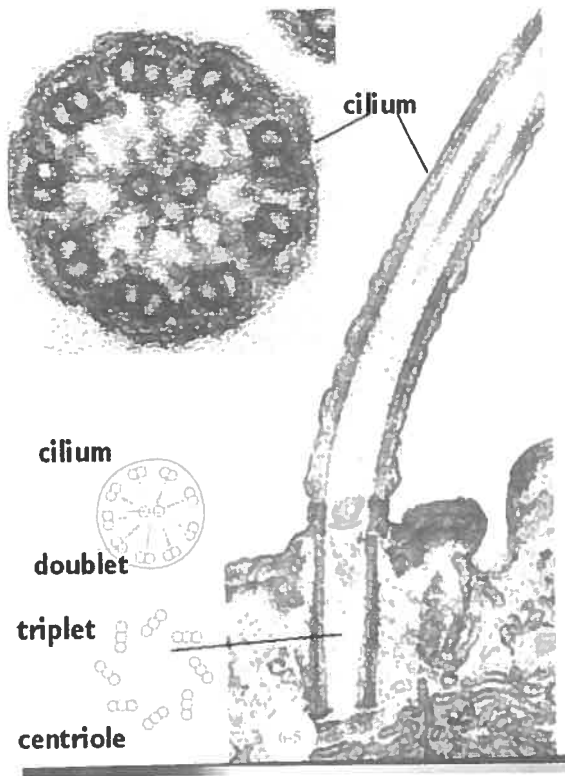


Figure 9

Gwen V. Childs, Ph.D.

<http://cellbio.utmb.edu/cellbio/cilia.htm>

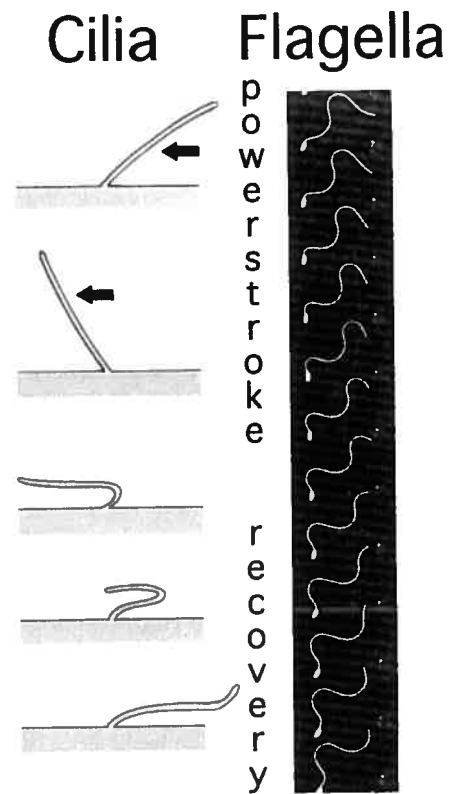
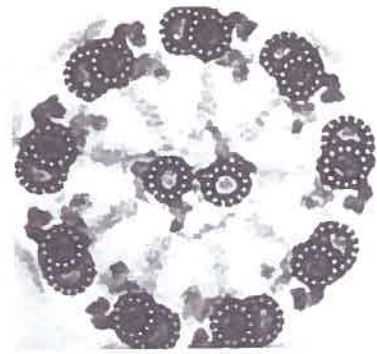
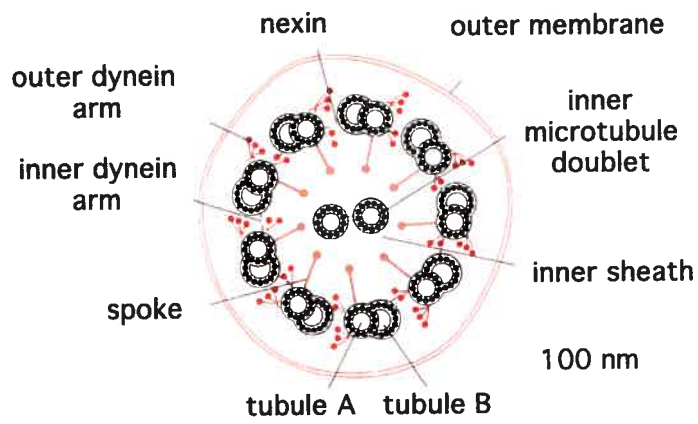


Figure 10



Gwen V. Childs, Ph.D.  
<http://cellbio.utmb.edu/cellbio/cilia.htm>

Figure 11

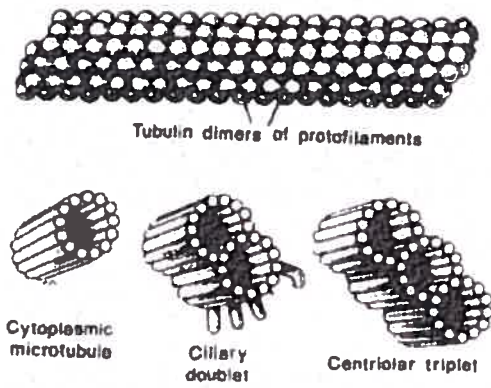


Figure 12

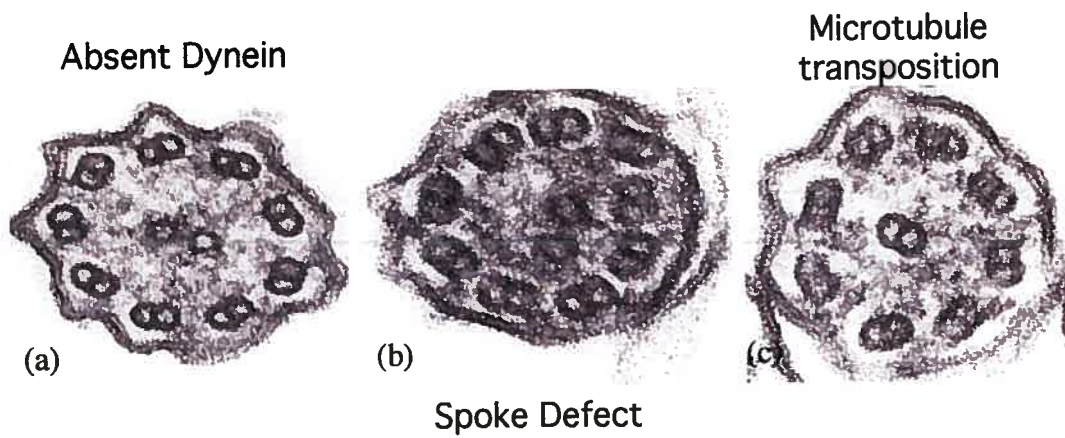


Figure 13

Nadel *et al*, Radiology 154: 651-655 (1985)